World Academy of Science, Engineering and Technology
International Journal of Energy and Power Engineering
Vol:5, No:8, 2011

Design, Simulation and Experimental Realization of Nonlinear Controller for GSC of DFIG System

R.K. Behera and S.Behera

***Abstract*—** In a wind power generator using doubly fed induction generator (DFIG), the three-phase pulse width modulation (PWM) voltage source converter (VSC) is used as grid side converter (GSC) and rotor side converter (RSC). The standard linear control laws proposed for GSC provides not only instablity against comparatively large-signal disturbances, but also the problem of stability due to uncertainty of load and variations in parameters. In this paper, a nonlinear controller is designed for grid side converter (GSC) of a DFIG for wind power application. The nonlinear controller is designed based on the input-output feedback linearization control method. The resulting closed-loop system ensures a sufficient stability region, make robust to variations in circuit parameters and also exhibits good transient response. Computer simulations and experimental results are presented to confirm the effectiveness of the proposed control strategy.

***Keywords*—**Doubly fed Induction Generator, grid side converter, machine side converter, dc link, feedback linearization.

I. Introduction

SEVERAL limitations associated with the squirrel cage induction generator and high costs of the permanent magnet synchronous generator (PMSG) can be overcome with the DFIG system. The basic diagram of DFIG system, which is shown in Fig.1, is capable of limited variable speed operation via a pair of back to back VSCs between the rotor circuit and the point of common coupling. Each of the VSCs typically consists of a pulse width modulated (PWM) IGBT-diode based phase legs. The rotor circuit of the DFIG is accessed via slip rings for connection to a voltage source converter (VSC), which is commonly referred to as the machine side converter (MSC). The stator circuit of the machine is connected to the grid via a step-up transformer, but without a power converter interface. The dc bus of the MSC feeds a VSC connected in parallel with the stator coils, commonly called the grid side converter (GSC) [1-3].

The dynamic modeling of DFIG, its operation during unbalanced conditions and its impact under influence of the disturbances have been analyzed [4-7]. For improving the performances, the various control strategies have been adopted to control the GSC in recent work [8-23]. The decupling/vector control technique has been considered [8] for independent control of variables. The controls of DFIG incase of unbalanced network supply and mitigation to disturbances have been investigated [9,10]. The PI controller in rotor circuit during variable speed is implemented [11], whereas the coordinated control and direct power control incase of network unbalance are implemented for better performances respectively [12-13,15]. The new controller known as TS-Fuzzy controller is included in DFIG to compare its effectiveness over conventional PI controller [14]. The stability analysis coupled with interarea oscillation damping and distorted grid voltage has been studied [16-17]. Qu et.al[18] proposed a different technique to derive constant power incase of variable speed with the help of supercapacitor energy storage. Mohesani et.al have developed a novel current regulator for DFIG to operate under unbalanced supply [19], whereas the new control techniques have been proposed to support the variable frequency as well as system's parameter variations [20,21]. In most cases, the researchers use linear control method to control over various abnormal operations such as unbalanced condition, change in parameters, torque pulsations, variable frequency etc. The linear control method, which is one of the powerful methods, has a long history of successful industrial applications. However, the linear control methods rely on the key assumption of small range operation for the linear plant model to be valid. Beyond the operation range, a linear controller is likely to perform very poorly or to be unstable, because the nonlinearities in the system cannot be properly compensated. Under such situation, a new method needs to be adopted so as to handle a nonlinear system in as simplified manner. So to handle such a nonlinear system, the researchers have already considered the feedback linearization technique [22,23] for improved performances of STATCOM, but the inclusion of this technique still lags incase of DFIG.

This paper proposes a nonlinear multivariable control technique based on feedback linearization theory for grid side control (GSC) of DFIG. One of the primary advantages of this

R.K.Behera is with Electrical Engg Dept, Indian Institute of Technology, Patna, INDIA (phone: +91-612-2552050; e-mail: rkb@iitp.ac.in).

S.Behera is with Instrumentation and Electronics Dept, College of Engineering and Technology, Bhubaneswar, INDIA (contact no: +91-9437420486; e-mail: sbehera@cet.edu.in).

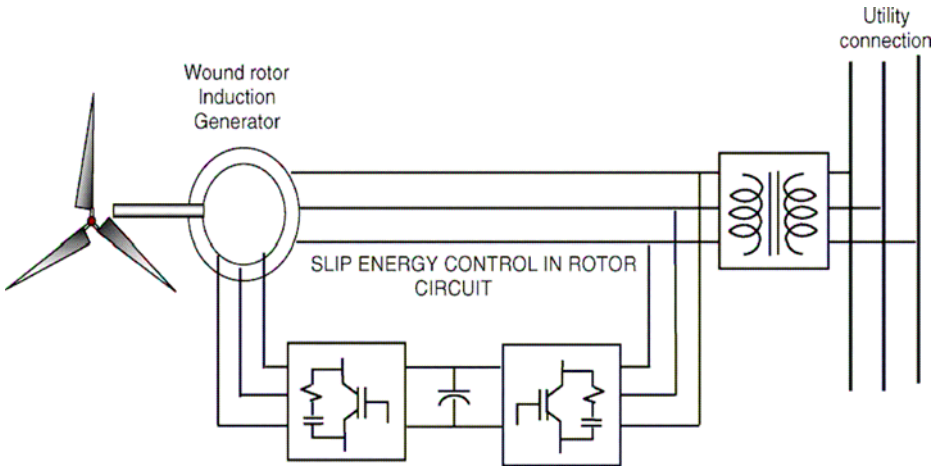

Fig.1: DFIG with bi-directional pulse with modulation converter

nonlinear controller is that it is robust to the variations in system or load parameters. The feedback linearization approach is based on the idea of canceling the nonlinearities of the system and imposing a desired linear dynamics to the control system. This nonlinear controller overcomes the disadvantages of the conventional linear controllers, keeping the dc-link voltage levels within their design limits, even during voltage dips resulting from abnormal grid voltage. Moreover, the study shows how the converter currents behave with respect to the poor behavior of standard PI controllers and the proposed nonlinear control technique.

II. Feedback Linearization Controller

The feedback linearization is achieved by exact state transforms and feedback, rather than by linear approximations of the dynamics. The main idea behind feedback linearization is the representation of the nonlinear system by means of a transformation and feedback in order to be able to obtain a linear relation between the input and output of the system. Thus, feedback linearization tries to cancel the system nonlinearities through the input of the system. After that, a desired dynamic can be imposed on the system by adding a new control input.

Consider that the multi-input multi-output (MIMO) nonlinear system, in the neighborhood of a point x0 is given by:

$$\dot{x} = f(x) + G(x)u \tag{1}$$

$$y = h(x). \tag{2}$$

This is commonly defined as a system, where x is the $n\times 1$ state vector, u is the $m\times 1$ control input vector (of component ui), y is the $m\times 1$ vector of system outputs (of component y_i), f and h are smooth vector fields, and G is a $n\times m$ matrix whose columns are smooth vector fields g_i.

Input-output linearization is obtained by differentiating the output y_i until the inputs appear. Assume that r_i is the smallest integer such that at least one of the inputs appears in $y_i(r_i)$, then

$$y_i^{(r_i)} = L_f^{\,r_i} h_i + \sum_{j=1}^{m} L_{gj} L_f^{\,r_i-1} h_i u_j. \tag{3}$$

with $L_{gj} L_f^{\,r_i-1} h_i(x) \neq 0$ for at least one j, in a neighborhood Ω_i of the point x_0. Performing the above procedure for each output y_i yields

$$\begin{bmatrix} y_1^{(r_1)} \\ .... \\ .... \\ y_m^{(r_m)} \end{bmatrix} = \begin{bmatrix} L_f^{\,r_1} h_1(x) \\ .... \\ .... \\ L_f^{\,r_1} h_1(x) \end{bmatrix} + E(x)u. \tag{4}$$

where $E(x)$ is $m\times m$ matrix and invertible.

In nonlinear control the relative degree is an important theoretical concept, which is related to the number of times that the system output yi has to be differentiated until the input u explicitly appears in the expression. The input

transformation can be written as

$$u = E^{-1}\begin{bmatrix} v_1 - L_f^{r_1} h_1 \\ .... \\ .... \\ v_m - L_f^{r_m} h_m \end{bmatrix}. \quad (5)$$

which yields m equations of the simple form

$$y_i^{(r_i)} = \gamma_i. \quad (6)$$

Since the new input γ_i only affects the output y_i. at this point, desired dynamics can be imposed on the system by the new system inputs through proper control design.

III. Nonlinear Control Application to Grid Side Converter Control

The schematic control block diagram of the GSC is shown in Fig. 2. Modeling of grid side converter in dq- reference frame is given in [2]. In matrix form it can be written as:

$$\frac{d}{dt}\begin{bmatrix} i_{sd} \\ i_{sq} \\ v_{dc} \end{bmatrix} = \begin{bmatrix} \frac{v_{sd}}{L_s} - \frac{R_s}{L_s} i_{sd} + \omega i_{sq} \\ \frac{v_{sq}}{L_s} - \frac{R_s}{L_s} i_{sq} + \omega i_{sd} \\ \frac{3}{2Cv_{dc}}(v_{sq} i_{sq}) - \frac{i_i}{C} \end{bmatrix} + \begin{bmatrix} 0 \\ \frac{-1}{L_s} \\ 0 \end{bmatrix} v_{iq} + \begin{bmatrix} \frac{-1}{L_s} \\ 0 \\ 0 \end{bmatrix} v_{id}. \quad (7)$$

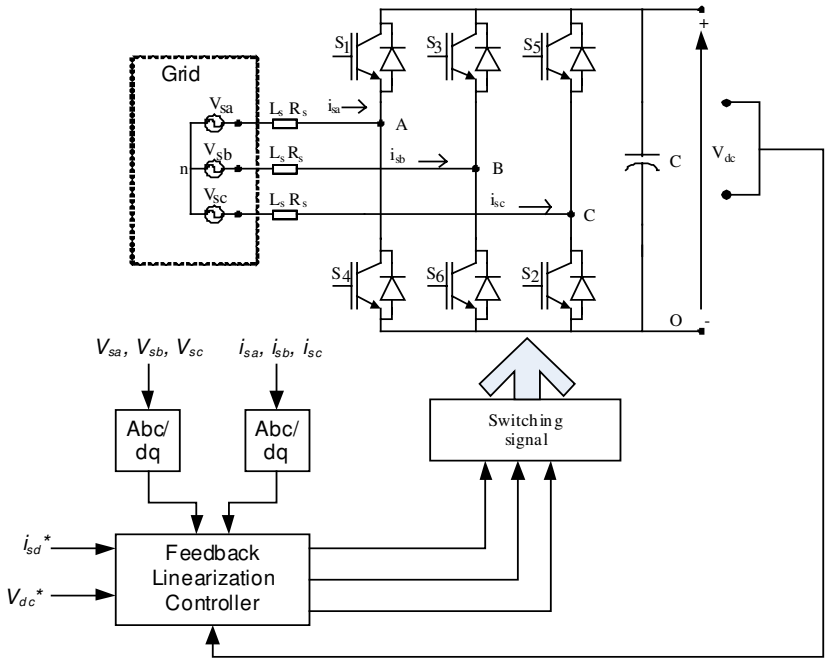

Fig. 2: Control block diagram of grid side converter (GSC)

Considering i_d and v_{dc} as the control output of the system.

$$y_1 = h_1(x) = i_{sd}$$
$$y_2 = h_2(x) = v_{dc}. \quad (8)$$

Now differentiating the output y_1 with respect to time:

$$\frac{d}{dt} i_{sd} = \frac{v_{sd}}{L_s} - \frac{R_s}{L_s} i_{sd} + \omega_s i_{sq} - \frac{1}{L_s} u_1. \quad (9)$$

Where $L_{g2}h_1 = 0$ and $u_1 = v_{id}$. The relative degree of this output is $r_1 = 1$. Now for the output y_2,

$$\dot{v}_{dc} = \frac{3}{2Cv_{dc}}(v_{sq} i_{sq}) - \frac{i_i}{C} \quad (10)$$

$$\ddot{y}_2 = L_f(L_f h_2) + L_{g1}(L_f h_2)u_1 + L_{g2}(L_f h_2)u_2$$
$$= \frac{3v_{sq}}{2Cv_{dc}}\left(\frac{v_{sq}}{L_s} - \frac{R_s}{L_s} i_{sq} + \omega i_{sd} - \frac{u_2}{L}\right) - \frac{3v_{sq} i_{sq}}{2Cv_{dc}^2}\left(\frac{3v_{sq} i_{sq}}{2Cv_{dc}} - \frac{i_i}{C}\right) - \frac{i_i}{C} \quad (11)$$

where $L_{g1}h_2 = 0$, $L_{g2}h_2 = 0$, $L_{g1}(L_f h_2) = 0$, and $u_2 = v_{iq}$. For this output the relative degree is $r_2 = 2$. The vector relative degree of the system is $r = (r_1, r_2) = (1, 2)$. Now, these equations can be rewritten in matrix form.

$$\begin{bmatrix}\dot{y}_1\\ \ddot{y}_2\end{bmatrix}=\begin{bmatrix}A_1\\ A_2\end{bmatrix}+E\begin{bmatrix}u_1\\ u_2\end{bmatrix} \tag{12}$$

$$A_1=\frac{v_{sd}}{L_s}-\frac{R_s}{L_s}i_{sd}+\omega_s i_{sq}$$

$$A_2=\frac{3v_{sq}}{2Cv_{dc}}(\frac{v_{sq}}{L_s}-\frac{R_s}{L_s}i_{sq}+\omega i_{sd})-\frac{3v_{sq}i_{sq}}{2Cv_{dc}^{\ 2}}(\frac{3v_{sq}i_{sq}}{2Cv_{dc}}-\frac{i_i}{C})-\frac{i_i}{C}$$

$$E=\begin{bmatrix}\frac{-1}{L_s} & 0\\ 0 & \frac{-3v_{sq}}{2L_sCv_{dc}}\end{bmatrix}. \tag{13}$$

Matrix E must be invertible. Now inverting E.

$$E^{-1}=\begin{bmatrix}-L_s & 0\\ 0 & \frac{-2L_sCv_{dc}}{3v_{sq}}\end{bmatrix}.$$

Therefore the control law is given by .

$$\begin{bmatrix}u_1\\ u_2\end{bmatrix}=E^{-1}(-\begin{bmatrix}A_1\\ A_2\end{bmatrix}+\begin{bmatrix}\gamma_1\\ \gamma_2\end{bmatrix}). \tag{14}$$

which lead to the input–output relation between the outputs $\dot{y}_i$ and the new inputs γ_i.

$$\begin{bmatrix}\dot{y}_1\\ \ddot{y}_2\end{bmatrix}=\begin{bmatrix}\gamma_1\\ \gamma_2\end{bmatrix}.$$

A desired dynamic response can be imposed using following:

$$\gamma_1=\dot{y}_1^*+\lambda_{10}(y_1^*-y_1) \tag{15}$$

$$\gamma_2=\ddot{y}_2^*+\lambda_{21}(\dot{y}_2^*-\dot{y}_2)+\lambda_{20}(y_2^*-y_2). \tag{16}$$

where $y^*_1= i^*_{sd}$, $y_1=i_{sd}$, $y^*_2=v^*_{dc}$, $y_2=v_{dc}$ are desired system response. The above equation cab be written as:

$$\dot{e}_1+\lambda_{10}e_1=0 \tag{17}$$

$$\ddot{e}_2+\lambda_{21}\dot{e}_2+\lambda_{20}e_2=0. \tag{18}$$

where $e_1=(y_1^*-y_1)$ and $e_2=(y_2^*-y_2)$.

Now (17) and (18) are stable for λ_{10}, λ_{21} and $\lambda_{20} > 0$. Then the exact controller can be formulated as

$$u_1=L(\frac{v_{sd}}{L_s}-\frac{R_s}{L_s}i_{sd}+\omega_s i_{sq}-\gamma_1) \tag{19}$$

$$u_2=\frac{2LCv_{dc}}{3v_{sq}}[\frac{3v_{sq}}{2Cv_{dc}}(\frac{v_{sq}}{L_s}-\frac{R_s}{L_s}i_{sq}+\omega i_{sd})-\frac{3v_{sq}i_{sq}}{2Cv_{dc}^{\ 2}}(\frac{3v_{sq}i_{sq}}{2Cv_{dc}}-\frac{i_i}{C})-\frac{i_1}{C}-\gamma_2] \tag{20}$$

As can be seen, using (19) and (20) can design be designed with appropriate values of λ_{10}, λ_{21} and λ_{20}.

IV. Simulation And Experimental Results

To validate the proposed feedback linearization controller for grid side converter control, the simulations are carried out using Matlab/simulink and a small experimental prototype is developed in the laboratory. The parameters of the grid side converter is given in Table I and feedback linearization controller is given in Table II [8]. The controller parameters λ_{10}, λ_{21} and λ_{20} were tuned to ensure that the dynamic response is faster and it is independent of parameters of the system. The GSC is simulated using MATLAB/Simulink and the results are shown below.

TABLE I
Grid Side Converters Parameters

Input supply phase voltage	480V (rms), 3 ph, 60 Hz.
DC link voltage	800 V
L_S	15 mH
R_S	0.4 Ω
C	1680 μF

TABLE II
Feedback Linearization Controller Parameters

Parameters	Value
λ_{10}	1000
λ_{21}	6500
λ_{20}	20000

This section presents the results of proposed input-output feedback linearization controller and comparison with linear controller. The results from simulations are shown in Figs 3~9 for both linear (PI controller) and nonlinear controller (i.e., with feedback linearization). In Figs 3(a) and 3(b), it shows the responses of I_{sq}, I_{sd} and I_{sdref} for linear and nonlinear controller respectively. Initially d-axis reference current is set to zero, then a step change of 4 A is applied at t = 1 s and subsequently a step change of -4 A is applied at t= 2 s. It is shown in Fig.3(a) that change in d-axis current is affecting q-axis current during transient condition. However, during

steady state, the d- and q-axis current control are perfectly decoupled. It is found that responses obtained with nonlinear controller (i.e., with feedback linearization) in Fig. 3(b) are much better as compared to Fig.3(a) of linear controller. Fig. 4 shows the voltage across the dc-link capacitor for both linear and nonlinear controller. Although dc-link voltage is settled at the reference voltage (800 V) during steady state but during transient it exhibits high peak overshoot in case of linear controller. This may lead to failure of the stability in controlled plant. In case of feedback linearization, the response of dc link voltage (i.e., Fig.4(b)) is found to be much better. The resultant grid side phase voltage and current is shown in Fig. 5 for linear controller and nonlinear controller. Fig. 5(a) shows the transition from unity power factor to leading power factor in case of linear controller. The input current waveform shows that when the grid side converter operates at leading power factor, it supplies reactive power to the source. It is confirmed that the current transient appears during transient condition and the settling time of the current response is high enough. With same situation of those in Fig.5(a), the results for nonlinear controller are presented in Fig. 5(b). In case of nonlinear controller, it is confirmed that there is no current transient appearing during transition period and the response time is fast enough. The simulation results confirm that the performance of the controller is independent of the system parameters and load and exhibits better performance over existing linear control system.

In order to realize the nonlinear control of GSC, an experimental setup is fabricated in laboratory. A Lab VIEW based digital processor that runs on National Instruments (NI) data acquisition system (PCI-MIO16-E-4), is employed for the control of GSC. The analog input sensor signals are sampled at the rate of 20 kHz/channel. A proportional plus integral controller is implemented using NI LabVIEW Real Time (RT) programming that carries out floating point operations required for the controller implementation. The three-phase converter bridge comprises three dual IGBT modules (SKM75GB128DN; 1200 V and 100 A). The output capacitor bank (Hitachi make, HCG F6A) has a rating of 3300 μF, 500 V dc. The power circuit is energized by increasing voltage through an autotransformer. The switching signals for IGBT's are then applied that results in usual operation of the GSC. Two current sensors (LA-55P) and a voltage sensor (LV-25P) are used and the signals are fed to A/D converter of the data acquisition card for control purpose. The relevant experimental results for GSC with nonlinear controller are given in Figs. 6-9 for the three-phase two-level converter system as shown in Fig. 1.

The d-axis and d-axis reference current using nonlinear controller is shown in Fig. 6. It is shown that the d-axis current is tracking perfectly the reference current. The current response during transient condition is also fast. The q-axis and d-axis current using nonlinear controller is shown in Fig. 7. It is shown that change in d-axis current does not affect q-axis current during transient condition. Thus d- and q-axes currents are perfectly decoupled. There is no over shoot during transient condition. So the decoupling control of active and reactive power is enhanced using nonlinear controller especially during transients. Fig. 8 shows the steady state result of A-phase voltage (Van) and current for unity power factor operation of GSC. Fig. 9 shows phase-A current during step change in magnitude of load current. Above all, this shows the improved dynamic performance of the GSC without any peak overshoot in the current transient.

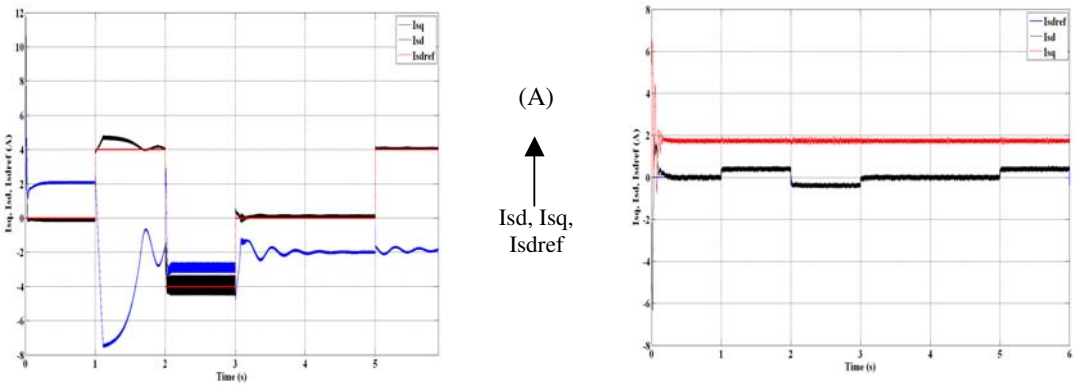

(a) (b)

Fig. 3. Response of Isq, Isd and Isdref with
(a) Linear controller (Isdref: red, Isd: black, Isq: blue)
Range X-axis: 0 to 6 sec, Range Y-axis: -8 to 10 A
(b) Non-linear controller. (Isdref: blue, Isd: black, Isq: red)
Range X-axis: 0 to 6 sec, Range Y: -8 to 8

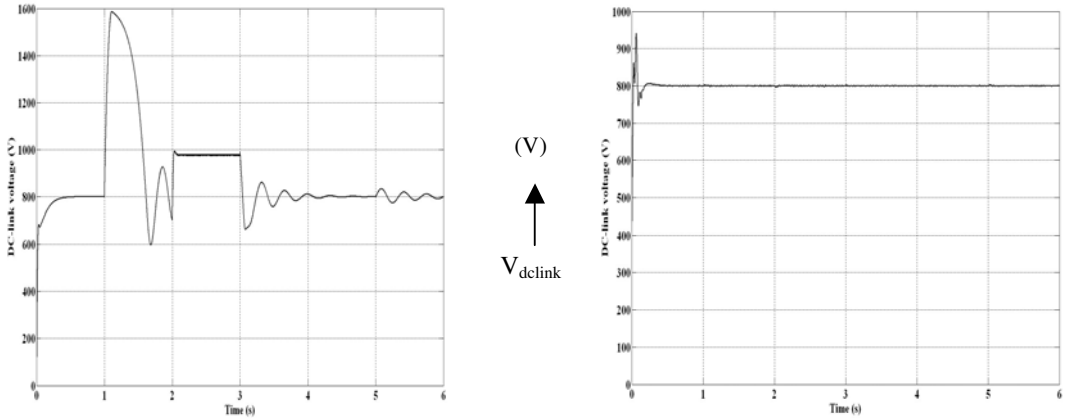

(a) (b)

Fig. 4. Response of dc-link voltage
(a) Linear controller (Y-axis: 0~1600 V)
(b) Nonlinear controller (Y-axis: 0~1000 V)
(X-axis (time): 0~6 sec)

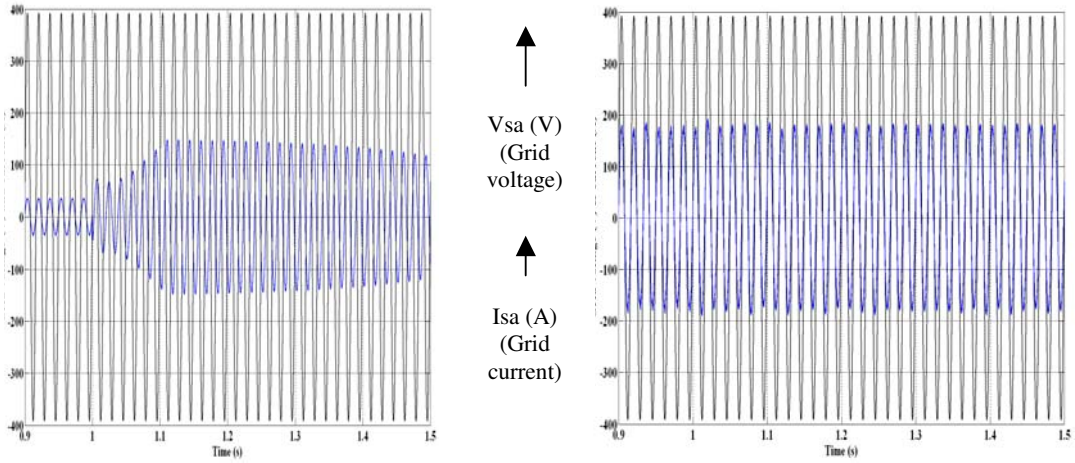

(a) (b)

Fig. 5. Grid voltage and current with Transition from unity pf to leading pf (Time: X-axis 0.9~1.5 sec,
Y-axis(range) : -400 to 400 ; Scale 1:1
(Grid voltage: black, current: blue)
(a) linear controller. (b) Nonlinear controller

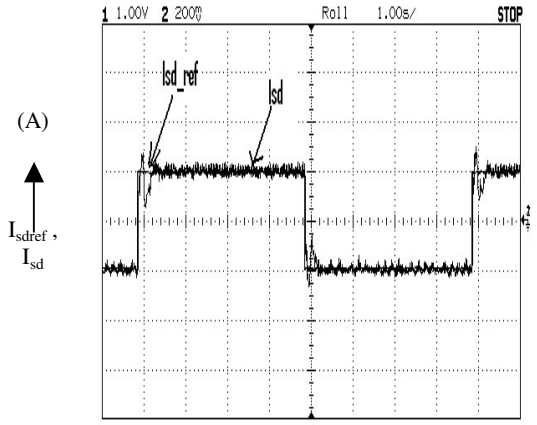

Fig. 6. Experimental results of I_{sd} and I_{sdref} with nonlinear controller.
Channel 1: I_{sdref}, d-axis reference current: 2 A/div., 1 s/div.
Channel 2: I_{sd}, d-axis current: 2 A/div., 1 s/div

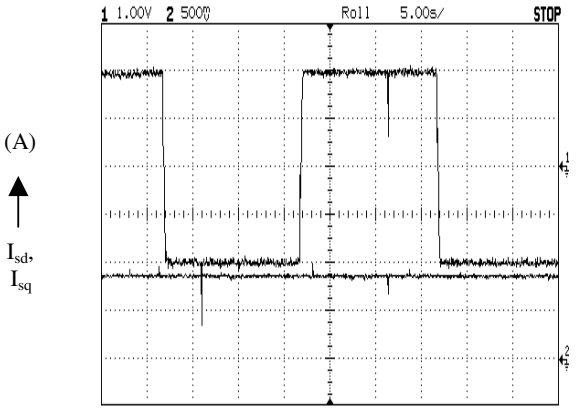

Fig. 7. Experimental results of I_{sd} and I_{sq} with nonlinear controller.
Channel 1: I_{sd}, d-axis current: 0.5 A/div.
Channel 2: I_{sq}, q-axis current: 1 A/div.

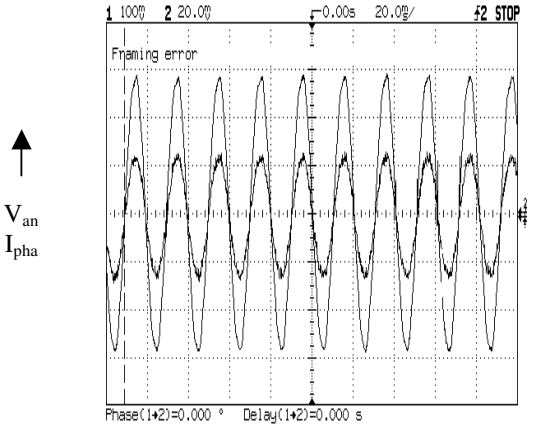

Fig.8. A-phase voltage and current with unity power factor:
Channel 1: Phase A voltage: 60V/div., 0.05 s/div.
Channel 2: Phase current: 1 A/div., 0.05 s/div.

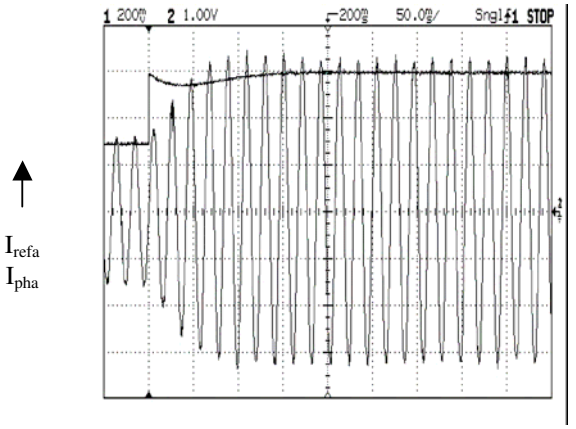

Fig. 9. A-phase current and step change in load current with unity power factor:
Channel 1: Reference Phase current: 0.5 A/div., 0.05 s/div.
Channel 2: Phase current: 1 A/div., 0.05 s/div.

V. Conclusion

The feedback linearization controller for the GSC is presented and found to be highly effective for the elimination of steady state errors, increasing the speed of response, and adding robustness against load and parameter variations. The comparison of the linear controller with the proposed feedback linearization controller shows that the later gives less error and exhibits faster than the linear controller. So the nonlinear controller has wide operating range and is stable against variations in load and system parameters. The performance obtained is quite encouraging and satisfactory.

REFERENCES

[1] S. Heier, Grid Integration of Wind Energy Conversion Systems, John Wiley & Sons, LTD., Chichester, England, 1998.

[2] R. Pena, J.C. Clare, G.M. Asher, "Doubly fed induction generator using back-to-back PWM converters and its application to variable-speed wind-energy generation," IEE Proc. Electric Power Applications, Vol. 143, No. 3, pp. 231 – 241, May. 1996.

[3] L. Holdsworth, X. G. Wu, J. B. Ekanayake, and N. Jenkins, "Comparison of fixed speed and doubly fed induction wind turbines during power system disturbances," Proc. Inst. Elect. Eng., vol. 150, no. 3, pp. 343–352, May 2003.

[4] L. Xu and Y. Wang, "Dynamic modeling and control of DFIG-based wind turbines under unbalanced network conditions," IEEE Trans. on Power Systems, vol. 22, Issue-1, pp. 314-323, Yr. 2007.

[5] M.K.Das, S.Chowdhury, S.P.Chowdhury and C.T. Gaunt, "Dynamics behaviour of a grid connected DFIG for wind energy conversion during disturbances," Universities Power Engineering Conference (UPEC), Proceedings of 44th International Publication, pp. 1-5, Yr. 2009.

[6] L.Shuhui, T.A. Haskew, and S.Mazari, "Integrating electrical and aerodynamic characteristics for DFIG speed control study, Power Sys. Conference and Exposition, PSCE-09, IEEE/PES, pp. 1-8, Yr. 2009.

[7] M. Kayikci and J.V. Milanovic, "Dynamic contribution of DFIG-based wind plants to system frequency disturbances," IEEE Trans. on Power Systems, vol. 24, Issue.2, pp. 859-867, Yr. 2009.

[8] L.Shuhui and T.A. Haskew, "Analysis of decoupled d-q vector control in DFIG Back-to-Back PWM Converter," IEEE Power Engineering Society General Meeting, pp. 1-7, Yr.-2007.

[9] Y.Wang and L.Xu, "Control of DFIG-based wind generation systems under unbalanced network supply," IEEE International Electric Machines and drives Conference, IEMDC'07," vol. 1, pp. 430-435, Yr. 2007.

[10] B.Pokharel and G. Wenzhong, "Mitigation of disturbances in DFIG-based wind farm connected to weak distribution using STATCOM," IEEE North American Power Symposium (NAPS)," pp. 1-7, Yr. 2010.

[11] G.Iwanski, and W.Koczara, "Rotor current PI controllers in the method of output voltage control of variable speed standalone DFIG," IEEE International Symposium on Industrial Electronics, ISIE-08, pp.2450-2455, Yr. 2008.

[12] L. Xu, "Coordinated control of DFIG's rotor and grid side converters during network unbalance," IEEE Trans on Power Electronics, vol. 23, Issue. 3, pp. 1041-1049, Yr. 2008.

[13] P. Zhou, Y.He and D.Sun, "Improved direct power control of a DFIG-based wind turbine network unbalance," IEEE Trans. on Power Systems, vol. 24, Issue-11, pp. 2465-2474, Yr. 2009.

[14] S.Mishra, Y.Mishra, L. Fangxing and Z.Y. Dong, "TS-Fuzzy controlled DFIG based wind energy conversion systems," IEEE Power & Energy Society General Meeting, PES'09, pp. 1-7, Yr. 2009.

[15] J. Kearney, M.F. Conlon and E.Coyle, "The integrated control of rotor side and grid side converters in a DFIG to reduce both power and torque pulsations during network voltage unbalance conditions," Proceedings of 44thInternational Universities Power Engineering Conference (UPEC), pp. 1-5, Yr. 2009.

[16] M.Zhixin, F.Lingling, D.Osborn and S.Yuvarajan, "Control of DFIG-Based wind generation to improve interarea oscillation damping, " IEEE Trans on Energy Conversion, vol.24, Issue. 2, pp. 415-422, Yr. 2009.

[17] J.Hu, H.Nian, H.Xu and Y.He, "Dynamic modeling and improved control of DFIG under distorted grid voltage conditions," IEEE Trans on Energy Conversion, Issue-99, pp. 1-13, Yr. 2010.

[18] L.Qu and W.Qiao, "Constant power control of DFIG wind turbines with supercapacitor energy storage," IEEE Trans. on Industry Appln, Issue-99, pp.1, Yr. 2010.

[19] M.Mohesani, M. Meshah, S.Islam and M.A.S. Masoum, "A novel current regulator for DFIG wind turbines with enhanced performance under unbalance supply," IEEE Power and Energy Society General Meeting, pp. 1-8, Yr. 2010.

[20] X. Zhang, H.Li and Y. Wang, "Control of DFIG-based wind farms of power network frequency support," International Conference on Power System Technology (POWERCON), pp. 1-6, Yr. 2010.

[21] J.P.DaCosta, H. Pinheiro, T.Degner and G.Arnold, "Robust controller for DFIG of grid connected wind turbines," IEEE Trans. on Industrial Electronics, Issue-99, pp. 1, Yr. 2010.

[22] N.C.Sahoo, B.K. Panigrahi, P.K. Dash and G.Panda, "Application of a multivariable feedback lineraization scheme for STATCOM Control," Electric Power Systems Research, Elesevier Publ. Pp. 81-92, Yr..2002.

[23] S.Mishra, B.K. Panigrahi and M.Tripathy, "A hybrid adaptive–bacterial–foraging and feedback linerization scheme based D-STATCOM," IEEE International conference on Power System Technology, POWERCON, pp. 1-6, Yr. 2004.

R.K.Behera received his both M.Tech and PhD from Indian Institute of Technology, Kanpur, INDIA in 2002 and 2007 respectively. At present he is with Department of Electrical Engg, Indian Institute of Technology, Patna. He is also Member of IEEE. His research area includes Power Electronics, Control and Drives.

S.Behera was born in Odisha, India on 9th June 1965. He received his M.Tech from Indian Institute of Technology, Kharagpur and PhD from Indian Institute of Technology, Kanpur in 1991 and 2003 respectively. At present he is working as Professor in Instrumentation and Electronics Engg, College of Engg and Technology, Bhubaneswar since 2009. He is also Member of IEEE. His research areas include AC/DC Drives, Power Quality, Instrumentation and Control.